International Journal of Microwave and Wireless Technologies

cambridge.org/mrf

Wideband tightly-coupled compact array of dipole antennas arranged in triangular lattice

Abhishek Kumar Awasthi and A. R. Harish

Department of Electrical Engineering, Indian Institute of Technology, Kanpur, Uttar Pradesh, India

Research Paper

Cite this article: Awasthi AK, Harish AR (2019). Wideband tightly-coupled compact array of dipole antennas arranged in triangular lattice. *International Journal of Microwave and Wireless Technologies* **11**, 382–389. https://doi.org/10.1017/S1759078718001605

Received: 30 May 2018
Revised: 12 November 2018
Accepted: 13 November 2018
First published online: 18 December 2018

Keywords:
Antenna array; antenna design; tightly coupled modeling and measurem

Author for correspondence:
A. K. Awasthi,
E-mail: abhishek.awasthi.ec@gmail.com

Abstract

In this paper, a compact wideband tightly-coupled dipole antenna array has been developed. Dipole elements are placed in the triangular lattice to reduce the side lobe level in the radiation pattern of one of the planes. To obtain the initial dimensions, 1-D infinite array analysis of the proposed array is carried out. The infinite array is designed to operate in 5–14.3 GHz (96.3% impedance bandwidth) frequency band. The antenna array can be used in C and X band applications. Inter-element coupling is utilized to achieve ultra-wideband performance in the proposed array. A 2×8 elements finite array is designed with the feed network. An ultra-wideband parallel strip to microstrip transition is used to feed the array elements. A metallic shielding for the feed network helps in reducing the back lobes. The overall size of the array with the reflector and the feed network is 148 mm × 224 mm × 54.5 mm. To validate the proposed concept, the antenna array is fabricated and tested. Impedance bandwidth of 2.8:1 along with broadside radiation pattern throughout the band of interest is observed.

Introduction

With new developments in communication systems and remote-sensing techniques, the need for ultra-wideband antenna array is also increasing. In recent years, a new methodology to design an antenna array is proposed, in which, mutual coupling between the elements of antenna array is used to improve the performance of the antenna array. The theoretical concept of the infinite connected array was proposed by Wheeler in 1965 [1]. Based on Wheeler's current sheet concept, Munk realized a practical continuous current aperture array [2], where inter-digital capacitor between the dipole edges is utilized to counteract the inductive behavior of the ground plane to obtain wideband performance. A wideband low-profile antenna array using long-slot aperture based on current sheet array was proposed by Lee *et al.* [3]. Later on, Lee *et al.* proposed a 10:1 wideband long-slot array with ferrite loaded ground plane [4]. A wideband wide-scan antenna array of connected dipoles was proposed by Cavallo *et al.* [5]. The array had 7×7 elements in which each element was fed with a loop-shaped transformer to avoid common-mode resonances. A wideband banyan tree antenna array has been proposed by Holland *et al.* [6]. The array employs a modular, low-profile structure which is directly fed by an unbalanced line. Shorting pins are utilized in the array design to reduce the common mode resonance. Further, Holland proposed 16×16 elements dual-polarized planar ultra-wideband modular antenna array that comprised tightly coupled dipole array [7]. Interwoven spiral array with a 10 : 1 bandwidth on a ground plane has been proposed by Tzanidis *et al.* [8]. Wideband performance is achieved via enhanced coupling due to inter-woven arms of the spiral. To model the radiation impedance of ultra-wideband antenna array with strong inter-element coupling, an equivalent circuit has been proposed by Alwan *et al.* [9]. A low-profile compact tightly-coupled array of the patch antennas was proposed by Irci *et al.* [10] where, the inter-element capacitance was obtained by the close proximity of the patch antennas which resulted in a very low-profile structure. A wideband antenna array with tightly coupled octagonal ring elements has been proposed by Chen *et al.* [11] where capacitive coupling between the elements is realized by the inter-digitizing the end portions of the ring elements. An ultra-wideband, wide scanning tightly-coupled dipole antenna array with integrated balun has been proposed by Doane *et al.* [12] in which the reactance of the compact Marchand balun is utilized as a matching network for each element. Moulder *et al.* [13] proposed a tightly coupled antenna array having a resistive frequency selective surface and a superstrate are utilized to enhance the performance of the antenna array. A wideband planner array with integrated feed and matching network with a non-symmetric tightly coupled dipole array has been proposed by Kasemodel *et al.* [14].

In various cases of the tightly-coupled antenna array, a large number of dummy elements are used to compensate for the edge elements performance. To enhance the performance of the edge elements, few techniques have been proposed. A method to design the excitation taper of finite size tightly coupled antenna array for efficient matching of all array elements has been proposed by Tazandis [15]. Later, Tazandis proposed a low profile tightly coupled

© Cambridge University Press and the European Microwave Association 2018

CAMBRIDGE UNIVERSITY PRESS

dipole array with an integrated balun in which different types of termination are used to enhance the performance of the finite array [16].

Most of the arrays reported in the literature using tight coupling technique havea large number of elements. With the infinite array analysis, the design of the tightly coupled array is computationally fast but is not accurate for small finite arrays. A small array of connected long-slot antenna [17] was proposed having optimized length and width of the feeding microstrip line for each port to match it with 50 Ω input impedance. A 2×8 elements tightly coupled antenna array with conjugative elements of a column printed on the opposite layer of the dielectric substrate has been presented in [18]. Due to the dual layer structure, the fabrication process is very complex in [18].

In this paper, a wideband, low-profile, compact (2×8 elements) array of tightly-coupled dipole antennas are proposed. In the proposed array, the triangular lattice is utilized to reduce side lobe level in one of the planes. Dipole is printed on the same layer of the substrate therefore, it reduces the fabrication complexity in the proposed array. The proposed array is basically designed for fan-type beam applications. Due to that, only two columns are used in this design. Coupling due to near-field radiation of the dipole elements along with the capacitive coupling between edges of dipoles is utilized to achieve ultra-wideband impedance bandwidth in the proposed array. Effect of the feed network on the performance of the tightly coupled antenna array is also discussed in this paper. Feed network of the proposed array is placed below the reflector and shielded by a metallic enclosure to reduce its effect on the performance of the array.

Analysis and design of proposed array

A unit cell of the proposed array is illustrated in Fig. 1. The structure is infinite in the *y*-direction and finite along *the x*-axis. Due to the triangular lattice, four dipoles are required to form the smallest repeating entity to be used as the unit cell of the proposed array. Dipoles are printed on the top layer of a substrate (Taconic TLY-5 $\varepsilon_r = 2.2$) of thickness *t*. Length and width of the dipole are l_d and w_d, respectively. Excitation gap between the dipoles is *g*. Along the *x*-direction, the dipoles are placed such that there exists a spacing *s* between the dipoles in the same row and two rows are placed with an offset of d_x. Inter-element spacing between the dipoles along the *y*-axis is d_y. A metallic reflector is placed at a distance of *h* below the substrate (Fig. 1(b)). Balun for each dipole is printed on a FR-4 substrate and connected to the dipole. Detailed structure of the balun and its assembly with the dipoles are presented in the section "Feed Network Design". Various dimensions of the unit cell are given in the caption of Fig. 1.

For the infinite array analysis, dipoles within the unit cell are excited simultaneously witha discrete port having source impedance of 175Ω. Balun is not used in this analysis. A comparison of the active reflection coefficient [19] of the elements of the unit cell, the reflection coefficient of element 1 of 2×2 finite array and the reflection coefficient of single isolated dipole element is shown in Fig. 8. In this paper, the reflection coefficient at the terminal of an element is computed or measured by terminating all other elements ina matched load and the active reflection coefficient is computed by exciting all other elements. Hence, the active reflection coefficient takes into account mutual coupling from all the elements and is more appropriate in case of the tightly coupled antenna array. Active reflection coefficient curves of port 3 and port 4 overlap with that of port 2 and port 1,

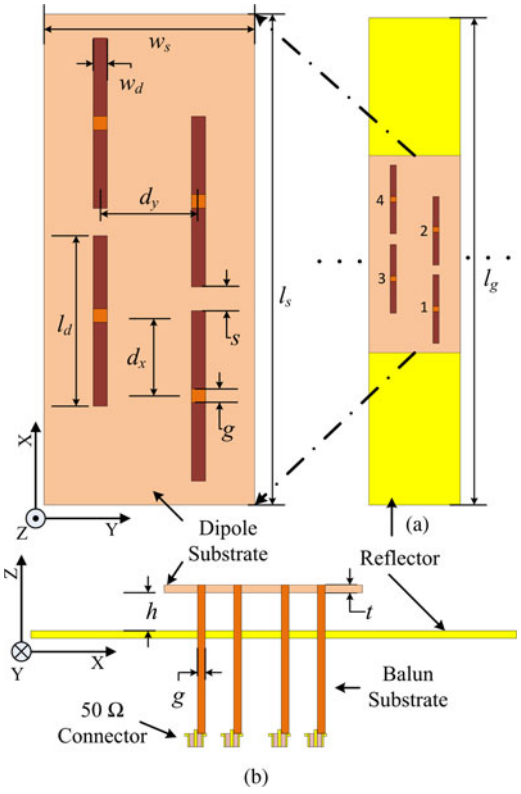

Fig. 1. Detailed geometry of the proposed unit cell, (a) Top view and (b) side view. $g = 1.6$, $d_y = 10.5$, $d_x = 9$, $l_d = 19$, $l_g = 121$, $l_s = 60.5$, $w_d = 1.35$, $w_s = 21$, $h = 6$, $s = 4$, and $t = 1.6$. All dimensions are in mm.

respectively. It is observed from the unit cell results that the ultra-wideband input impedance bandwidth is achieved from simple dipole elements by utilizing high inter-element coupling.

Infinite array analysis

To analyze the behavior of the proposed array, a parametric analysis of the unit cell is carried out. Let f_{L1} and f_{L2} be the lower − 10 dB band-edge frequencies of the active reflection coefficient at port 1 and port 2, respectively. Similarly, f_{H1} and f_{H2} be the upper − 10 dB band-edge frequencies at port 1 and port 2, respectively. These band edge frequencies are marked in Fig. 8. Fig. 3 shows the variation of the lower and upper band edge frequencies with respect to various design parameters. Effect of variation in dipole length l_d on the band edge frequencies is shown in Fig. 3(a). By increasing l_d, the lower cut off frequencies are decreasing while there is almost no effect on the upper cut off frequencies. Thus, we can conclude that by increasing the dipole length, bandwidth of the proposed array can be increased. It is observed from Fig. 3(b) that by increasing dipole width w_d, the upper band edge frequencies are increasing proportionally, while the lower band edge frequencies are unaffected, which also concludes that wider dipole gives wider impedance bandwidth. The feed gap also affects the upper band edge frequency more than the lower edge frequency. Lower value of feed gap results in wider bandwidth (Fig. 3(c)). Offset d_x is used to create the triangular lattice in the proposed array. Effect of variation in d_x is shown in Fig. 1(d). When there is no offset, i.e. rectangular lattice, the band edge frequency for port 1 and port 2 are same. Offset affects the band edge frequencies, but the bandwidth of the proposed array itself does not change with d_x.

https://doi.org/10.1017/S1759078718001605 Published online by Cambridge University Press

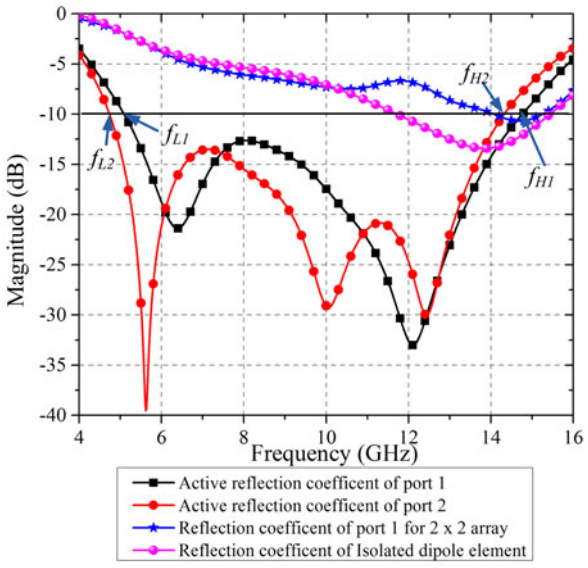

Fig. 2. Reflection coefficient of the array elements for various configurations.

Ultra-wideband performance of the proposed array is achieved by utilizing high inter-element coupling. There are two types of mutual interactions present in the proposed array. First, the coupling due to near-field radiation of the antenna elements and second the capacitive coupling between the edges of the dipole of the same row.

To verify this, the effect of variation in the inter-element spacing d_y and dipole edge gap s are analyzed for an infinite array. These two parameters control the inter-element coupling in the proposed array. Active reflection coefficient at port 1 for different values of s is shown in Fig. 4(a). For the smaller value of s, the bandwidth of the array is large but active reflection coefficient at the mid frequencies is nearly touching -10 dB. Therefore, the value of s is to be chosen properly to achieve wider bandwidth with a good input impedance match over the entire band. Effect of inter-element spacing d_y on the performance of the proposed array is shown in Fig. 4(b). As d_y increases, the mutual coupling between the dipoles decreases which reduces the impedance bandwidth of the proposed array. Same can be observed from the parametric results that by increasing d_y, the lower and upper band edge frequencies are approaching towards each other which results in the reduction in the impedance bandwidth.

Finite array analysis

The layout of 2×8 elements finite array with the element numbers is shown in Fig. 5. Various properties of the proposed finite array without feed network are analyzed in this section.

The proposed array has certain symmetries and hence, various results of the finite array are discussed only for half the number of elements (element 1 to element 8). Active reflection coefficients for different elements of finite array are shown in Fig. 6 (a). Due to the small size of the array, the active reflection coefficient of array elements is different for inner and edge elements. Instead of making the performance of every element identical, it is easier to make the operating band of each element same. Variation of the active reflection coefficient with frequency could be different for each of the elements. To observe coupling between the elements of the finite array, the elements are excited individually

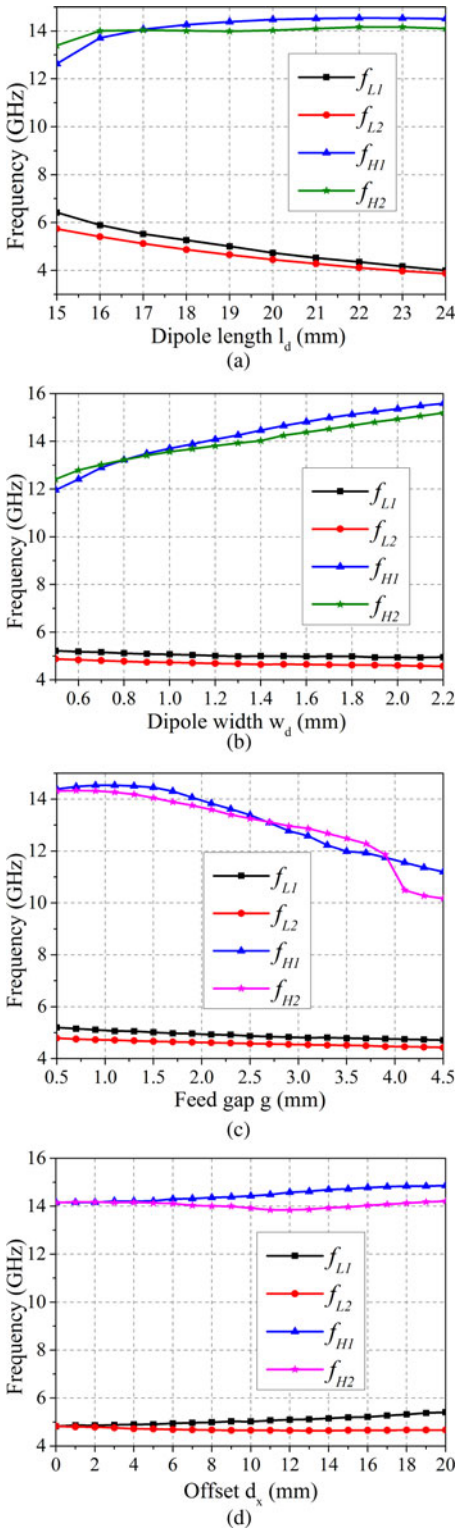

Fig. 3. Lower and upper band edge frequency variation with respect to various design parameters, (a) Dipole length, (b) Dipole width, (c) Dipole feed gap and (d) Offset d_x.

and complete scattering matrix of the array is obtained. The reflection coefficient of the element 8 and its coupling with the rest of the elements are shown in Fig. 6(b). It is observed from the results that the impedance bandwidth of the element without taking mutual coupling into account isa narrow band in nature. Mutual coupling for the inner element (say element 8) is high

https://doi.org/10.1017/S1759078718001605 Published online by Cambridge University Press

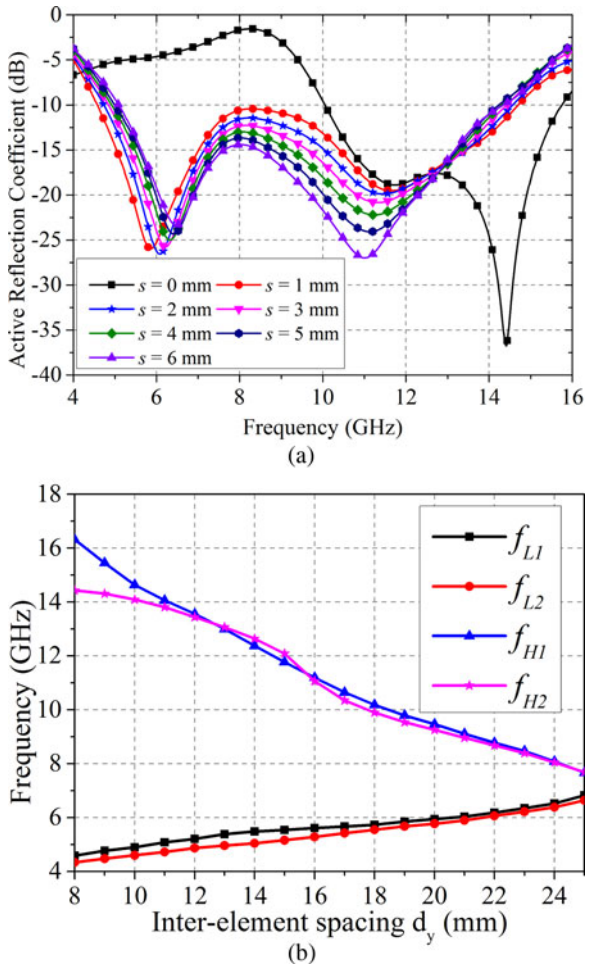

Fig. 4. Effect of inter-element coupling on the performance of the proposed array, (a) variation of dipole edge gap s and (b) variation in inter-element spacing d_y.

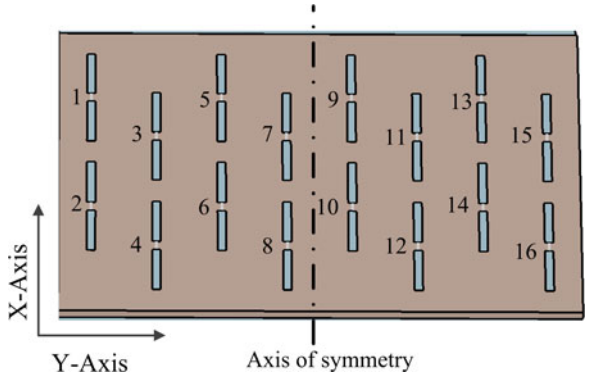

Fig. 5. The layout of 2 × 8 finite array.

for the closer elements and it is gradually decreasing as the distance between the elements is increasing.

To demonstrate the advantage of using a triangular lattice, the radiation properties of a rectangular lattice array are compared with the proposed triangular lattice array. Rectangular lattice array is just created by setting offset $d_x = 0$ and rest of the dimensions are the same in both the arrays. Side lobe level for the proposed and rectangular lattice arrays in both XZ and Y

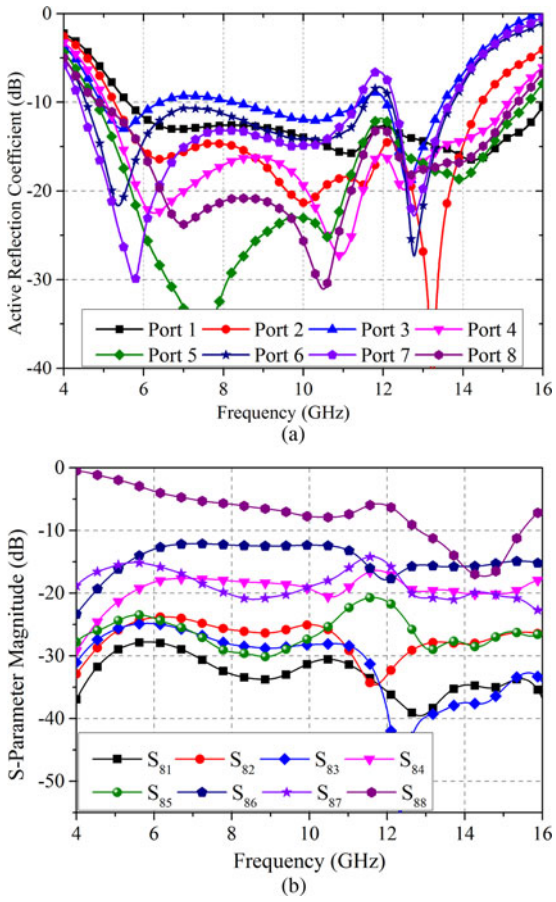

Fig. 6. Reflection coefficient of the proposed array (a) active reflection coefficient of the finite antenna array (all elements are excited) and (b) reflection coefficient of element 8 and its coupling to other element (only 8th element is excited rest of the elements are terminated in matched load).

Z planes are shown in Fig. 7(a). In the XZ-plane, side lobe level is improved for the triangular lattice compared with rectangular lattice. In the Y Z-plane, there is no effect on the side lobe level by varying the lattice from rectangular to triangular. To solve the high side lobe problem without affecting the impedance bandwidth of the array, use of the triangular lattice is a good option. The total efficiency of the finite array, as shown in Fig. 7(b), is better than 90% over the band of interest. The realized gain and the aperture efficiency of the proposed antenna array is shown in Fig. 8. The realized gain of the array is nearly constant over the frequency band of the interest. At low-frequency operations, the aperture efficiency is high. It decreases with the frequency. Over the band of interest, more than 50% aperture efficiency is obtained.

Feed network design

In the previous sections, discrete ports of 175 Ω are used to analyze the finite array. To physically test the array, we need to excite the array using 50 Ω coaxial lines. For this, an ultra-wideband feed network is required. In this section, an ultra-wide band feed network along with proposed 2 × 8 finite array is studied. The feed network consists of 16 individual feeds. For each element, a parallel strip to microstrip line UWB balun is designed to provide 175 Ω to 50 Ω impedance transformation. Thegeometry

https://doi.org/10.1017/S1759078718001605 Published online by Cambridge University Press

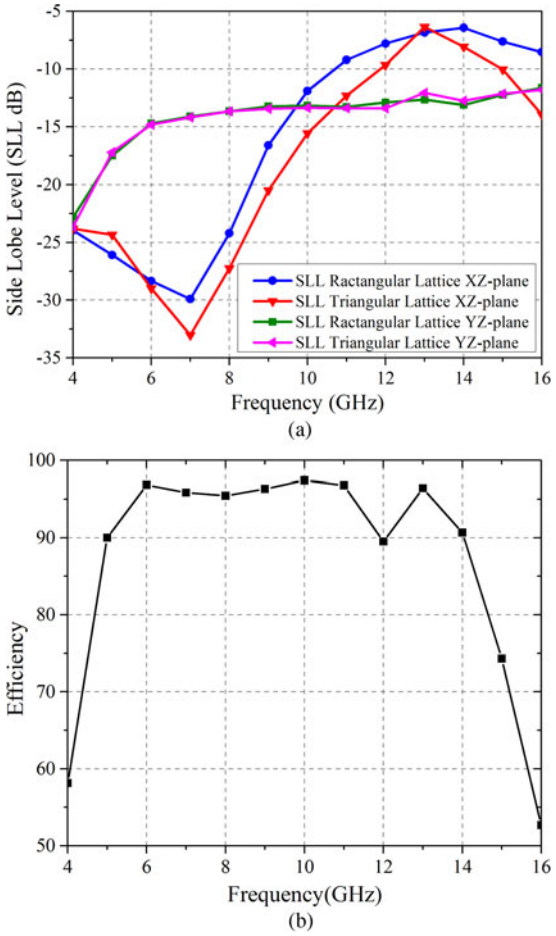

Fig. 7. Side lobe level and efficiency of the finite array (a) Comparison of side lobe level of proposed triangular lattice with rectangular lattice and (b) Total efficiency.

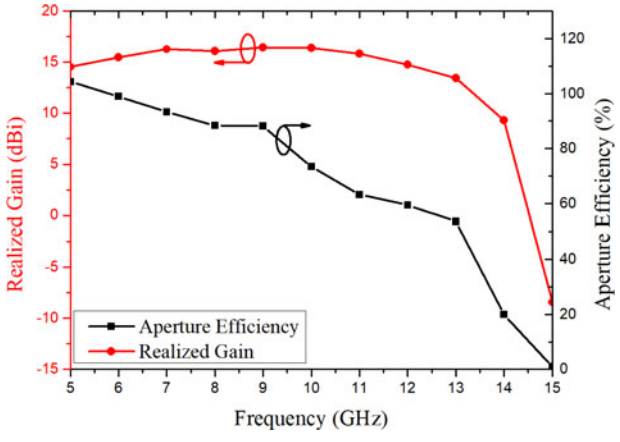

Fig. 8. Realized gain and aperture efficiency of the proposed antenna array.

of the feed network element is illustrated in Fig. 9(a). To implement the balun, FR-4 ($\varepsilon_r = 4.4$) substrate is used. Wave port excitation for each port is chosen in the simulation of the balun. The magnitude of the S-parameters of the balun is shown in Fig. 9(b). It can be observed from the results that the performance of the balun is good over 2–20 GHz frequency band. Due to the lossy

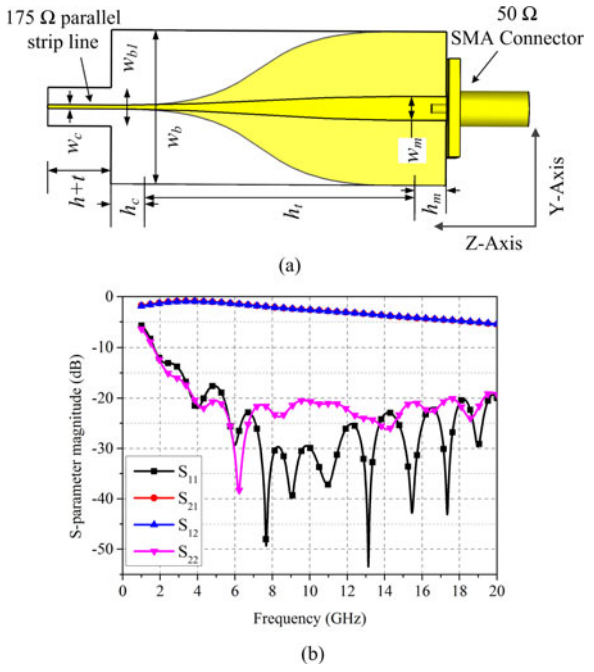

Fig. 9. Feed network element, (a) Geometry of parallel strip to microstrip balun and (b) magnitude of S-parameters of balun. Various dimensions of balun are as follows: $w_c = 0.5$, $w_m = 3.1$, $w_b = 20$, $w_{b1} = 5$, $h_c = 2$, $h_m = 7$, $h_t = 36$, $h = 6$, $t = 1.6$. All dimensions are in mm.

nature of FR-4 substrate, high insertion loss at the higher frequencies is observed. Various dimensions of the balun are given in the caption of Fig. 9.

The feed network is arranged in such a way that its presence will havea minimum effect on the performance of the array. To achieve this, a section of parallel strip line on a narrow substrate is extended over the balun. The wider section of the substrate is placed below the reflector of the antenna array. However, the narrow section passes through the reflector and the dipole substrate and is connected to the dipoles. From Fig. 5, it can be observed that there are four dipoles in one column. Although the array is 2×8 in nature, due to the triangular lattice, these dipoles are arranged in four columns. Four baluns are printed on a single substrate to feed four dipoles ofa single column. The position of the baluns for the adjacent columns is shifted by distance d_y. Assembly of the feed network is shown in Fig. 10(a). Spacers are used to maintain the proper distance between the balun substrates. The metallic reflector is placed over the feed network and the extended parallel strip lines pass through the holes of diameter w_{b1} in the reflector. Complete assembly of the array is shown in Fig. 10(b). Plexiglas spacers of height h are used at the edges ofa substrate on which dipoles are printed to provide uniform support and spacing between the substrate and the reflector. Rectangular openings of length g_1 and width w_{b1} are created in the dipole substrate for the extended parallel strip line. The major effect of the feed network on the performance of the antenna array is due to the holes in the metallic reflector made for the extended parallel strip line. Back lobe is observed in the radiation pattern of the array due to these holes. A metallic shield, as shownin Fig. 10(b), is used to suppress the back lobe. Final dimensions of the array are optimized with the complete feed network and given in the caption of Fig. 10.

https://doi.org/10.1017/S1759078718001605 Published online by Cambridge University Press

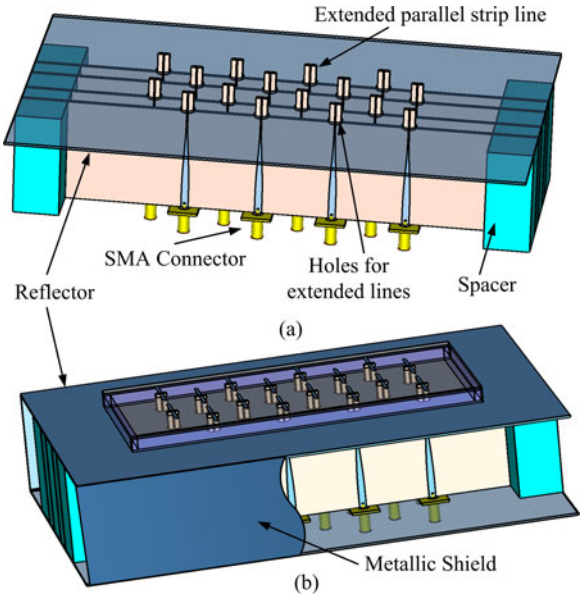

Fig. 10. Different building blocks of proposed array, (a) complete feed network with SMA connectors and (b) complete assembled proposed array. Final optimized dimension of the array with feed network is as follows. $g = 1.6$, $d_y = 16$, $d_x = 12$, $l_d = 23$, $w_d = 1.5$, $h = 6$, $s = 5$, and $t = 1.6$. All dimensions are in mm.

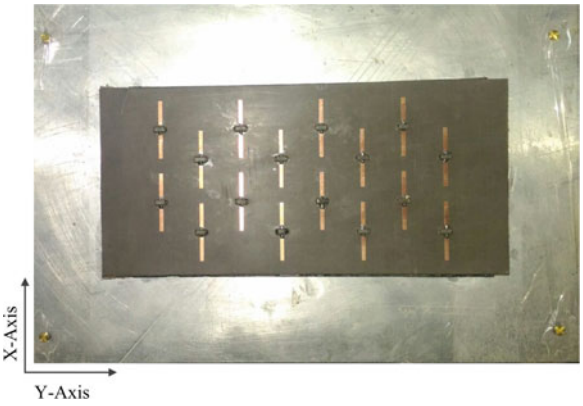

Fig. 11. Fabricated prototype of proposed array.

Results and discussion

To validate the proposed antenna array as discussed in the previous sections, a 2×8 elements finite array is fabricated and tested. A fabricated prototype of the proposed array is shown in Fig. 11. To compute the active reflection coefficient of the fabricated antenna array, reflection coefficient of all elements and their coupling with all other elements are measured. This is carried out by connecting two ports of the antenna array to the network analyzer while the rest of the elements are terminated with the matched load. Measurement for all the combination is done to complete the 16×16 scattering matrix of the fabricated 16 port antenna array. Further, the active reflection coefficient is computed from the measured scattering matrix by the use of equation (1) [20].

$$\{S_i\}_{active} = [S]\{V_i\}_{excitation}, \quad (1)$$

where $\{V_i\}_{excitation}$ is the excitation coefficient vector and $[S]$ is measured scattering matrix.

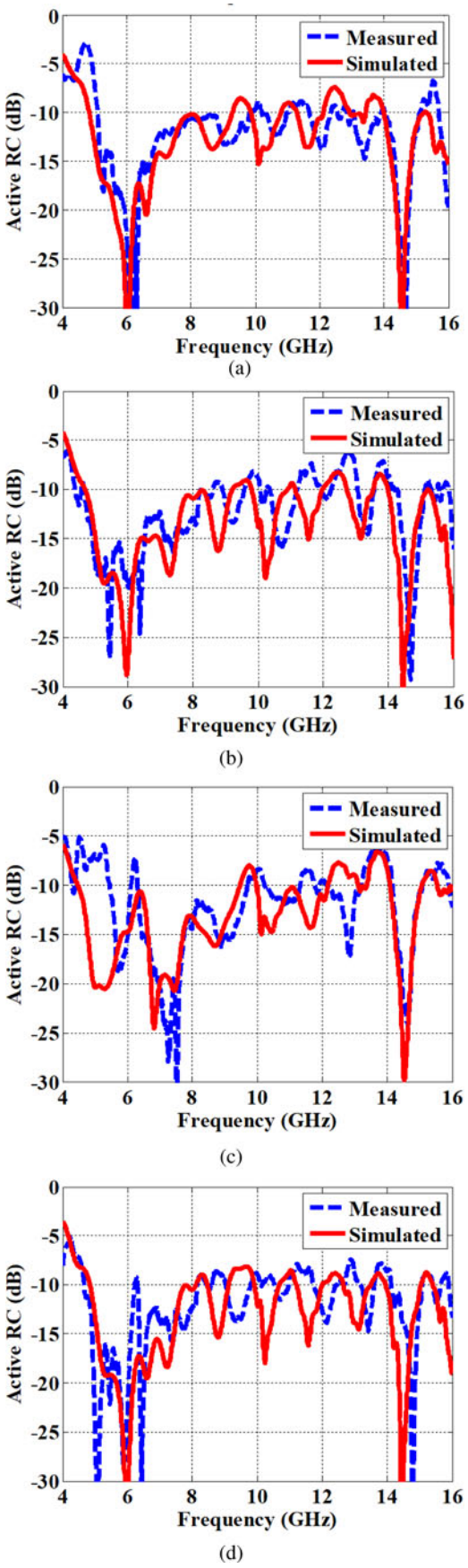

Fig. 12. Measured and simulated active reflection coefficient of the proposed array, (a) port 1, (b) port 3, (c) port 5, and (d) port 7.

https://doi.org/10.1017/S1759078718001605 Published online by Cambridge University Press

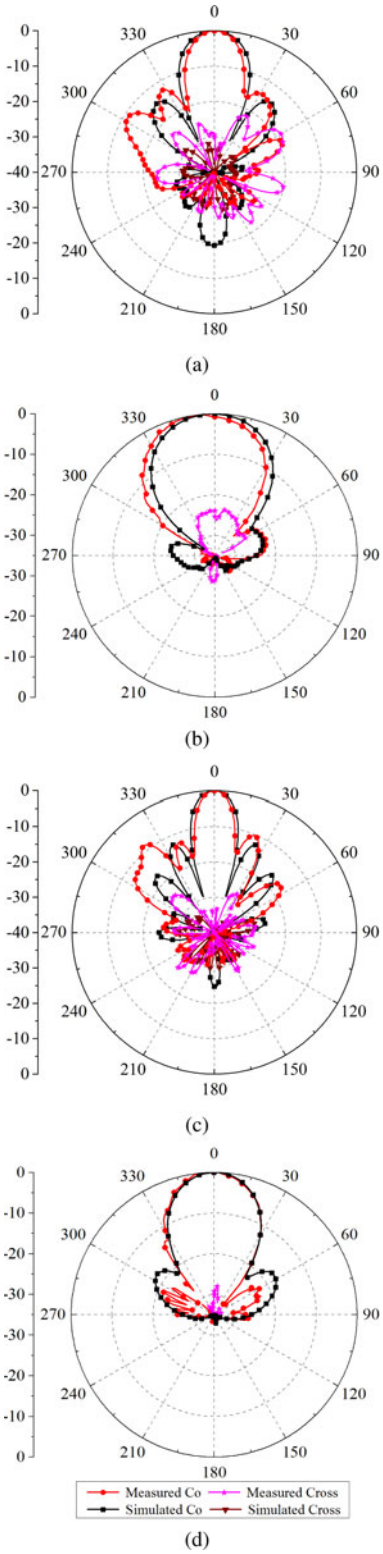

Fig. 13. Measured and simulated radiation pattern of the proposed array in *XZ* and *Y Z* plane, (a) 5 GHz *Y Z*-plane, (b) 5 GHz *XZ*-plane, (c) 8 GHz *Y Z*-plane, and (d) 8 GHz *XZ*-plane.

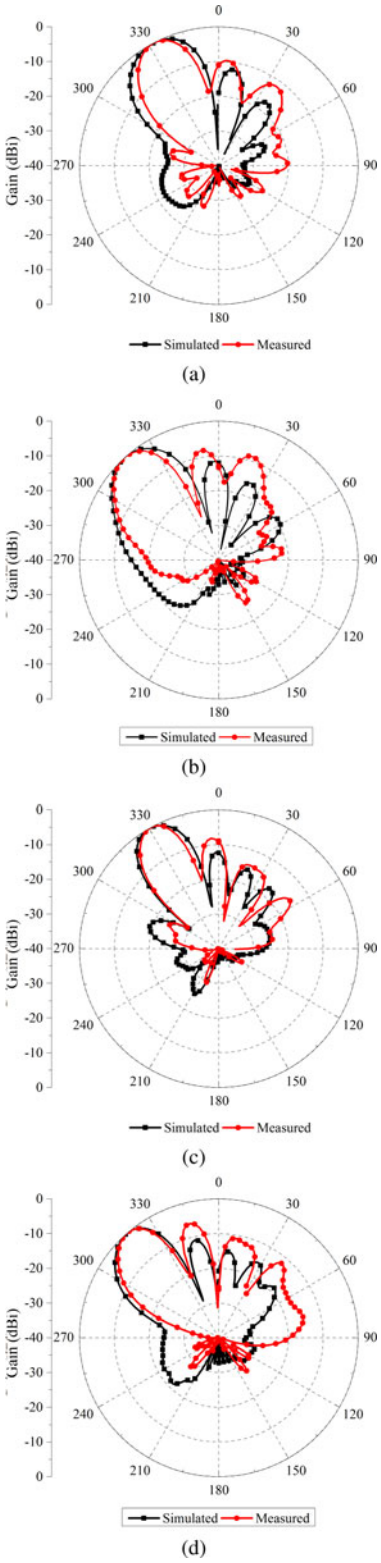

Fig. 14. Measured and simulated beam scanning pattern of the proposed array, (a) 5 GHz – 30° scan, (b) 5 GHz – 45° scan, (c) 7 GHz – 30° scan, and (d) 7 GHz – 45° scan.

In this case, uniform excitation without any phase shift is used to compute the active reflection coefficient. To compute active reflection coefficient for any particular scan angle, appropriate progressive phase shift can be introduced in the excitation coefficient vector. Measured and simulated active reflection coefficients of the antenna array are plotted in Fig. 12. A good match between the measured and simulated active reflection coefficient of the proposed array is obtained. To obtain the radiation pattern of the fabricated antenna array, active element pattern [21] of

https://doi.org/10.1017/S1759078718001605 Published online by Cambridge University Press

each element is measured by connecting the transmitter to one of the elements and terminating all other elements ina matched load. The vector sum of all active element patterns is used to compute the measured radiation pattern of the proposed antenna array. Fig. 13 shows the measured and simulated radiation pattern of the proposed antenna array in *XZ*-plane and *Y Z*-plane. Broadside gain of the proposed antenna array for 5 and 8 GHz are 14.7 and 16.4 dBi, respectively. There is good agreement between measured and simulated pattern along the main beam. There are some discrepancies in the side lobe measurement results. Error in measurement could be due to the dimensional errors which occur because of the manufacturing tolerance. This affects the measured phase which in turn hasa significant influence on the side lobe performance of the array. The second issue is with the measurement setup of the fabricated array. To do vector sum of active element patterns, both magnitude and the phase are needed to be measured. Even small errors in phase measurement badly affect the side lobe performance of the fabricated antenna array. Measured and simulated radiation pattern of the proposed antenna array for different scan angles are shown in Fig. 14. The patterns for 30° and 45° scan angle are plotted for 5 and 7 GHz. A significant good match is observed between the measured and simulated results. The gain of the patterns shown in Fig. 14(a), Fig. 14(b), Fig. 14(c), and Fig. 14(d) are 14, 13.9, 15.5, and 14.5 dBi, respectively.

Conclusion

A compact wideband 2×8 elements tightly-coupled antenna array is presented. By the utilization of the triangular lattice 3–4 db reduction in the side lobe level of the *XZ*-plane pattern is observed. The efficiency is more than 90% over the band of operation of the antenna array. From the proposed array 2.8:1 impedance bandwidth is obtained. Excellent radiation characteristics are observed over the entire frequency band of interest. A good match between measured and simulated results is observed.

Author ORCIDs. Abhishek Kumar Awasthi 0000-0003-4880-9733

References

1 **Wheeler H** (1965) Simple relations derived from a phased-array antenna made of an infinite current sheet. *IEEE Transactions on Antennas and Propagation* **13**, 506–514.
2 **Munk BA** (2003) *Finite Antenna Arrays and FSS*. Wiley-Interscience, USA.
3 **Lee JJ, Livingston S, Koenig R, Nagata D and Lai LL** (2006) Compact light weight UHF arrays using long slot apertures. *IEEE Transactions on Antennas and Propagation* **54**, 2009–2015.
4 **Lee JJ, Livingston S and Nagata D** (2008) A low profile 10:1 (200-2000 MHz) wide band long slot array. *IEEE Antennas and Propagation Society International Symposium, San Diego*.
5 **Cavallo D, Neto A, Gerini G, Micco A and Galdi V** (2013) A 3- to 5-GHz wideband array of connected dipoles with low cross polarization and wide-scan capability. *IEEE Transactions on Antennas and Propagation* **61**, 1148–1154.
6 **Holland SS, Vouvakis MN** (2011) The banyan tree antenna array. *IEEE Transactions on Antennas and Propagation* **59**, 4060–4070.
7 **Holland SS, Schaubert DH and Vouvakis MN** (2012) A 721 GHz dualpolarized planar ultrawideband modular antenna (PUMA) array. *IEEE Transactions on Antennas and Propagation* **60**, 4589–4600.
8 **Tzanidis I, Sertel K and Volakis JL** (2011) An interwoven spiral array (ISPA) with a 10:1 bandwidth on a ground plane. *IEEE Antennas and Wireless Propagation Letters* **10**, 115–118.
9 **Alwan EA, Sertel K and Volakis JL** (2012) A simple equivalent circuit model for ultrawideband coupled arrays. *IEEE Antennas and Wireless Propagation Letters* **11**, 117–120.
10 **Irci E, Sertel K and Volakis JL** (2011) An extremely low profile, compact, and broadband tightly coupled patch array. *Radio Science* **47**, 1–13.
11 **Chen Y, Yang S and Nie Z** (2012) A novel wideband antenna array with tightly coupled octagonal ring elements. *Progress In Electromagnetics Research* **124**, 55–70.
12 **Doane JP, Sertel K and Volakis JL** (2013) A wideband, wide scanning tightly coupled dipole array with integrated balun (TCDA-IB). *IEEE Transactions on Antennas and Propagation* **61**, 4538–4548.
13 **Moulder WF, Sertel K and Volakis JL** (2012) Superstrate-enhanced ultrawideband tightly coupled array with resistive FSS. *IEEE Transactions on Antennas and Propagation* **60**, 4166–4172.
14 **Kasemodel JA, Chen CC and Volakis JL** (2013) Wideband planar array with integrated feed and matching network for wide-angle scanning. *IEEE Transactions on Antennas and Propagation* **61**, 4528–4537.
15 **Tzanidis I, Sertel K and Volakis JL** (2012) Characteristic excitation taper for ultrawideband tightly coupled antenna arrays. *IEEE Transactions on Antennas and Propagation* **60**, 1777–1784.
16 **Tzanidis I, Sertel K and Volakis JL** (2013) UWB low-profile tightly coupled dipole array with integrated balun and edge terminations. *IEEE Transactions on Antennas and Propagation* **61**, 3017–3025.
17 **Awasthi AK and Harish AR** (2015) Low complexity feed system for a long slot antenna array, *IEEE International Symposium on Antennas and Propagation and USNC/URSI National Radio Science Meeting, Vancouver*.
18 **Awasthi AK and Harish AR** (2016) Wideband low profile tightly coupled dipole antenna array with an integrated balun, *International Conference on Emerging Trends in Communication Technologies (ETCT), Dehradun, India*.
19 **IEEE standard for definitions of terms for Antennas,** IEEE Std 145-2013 (Revision of IEEE Std 145-1993), (2014),pp. 1–50.
20 **Kalfa M and Halavut E** (2013) A fast method for obtaining active S-parameters in large uniform phased array antennas, *IEEE Int. Symp. on Phased Array Systems and Technology, Waltham*.
21 **Pozar DM** (1965) The active element pattern. *IEEE Transactions on Antennas and Propagation* **42**, 1176–1178.

Abhishek K. Awasthi did B.Tech. in electronics and communication from Uttar Pradesh Technical University (UPTU), Lucknow in 2008. He received his M.Tech. degree in digital communication from GGSIP University, Delhi in 2011. He received his doctoral degree from the Department of Electrical Engineering of Indian Institute of Technology Kanpur. He is currently an assistant professor with the Department of Electronics and Communication Engineering, Amity University Jharkhand Ranchi. His current research interests include antenna array analysis and microwave measurement.

A. R. Harish received the Ph.D. in Electrical Engineering from the Indian Institute of Technology Kanpur, Kanpur, India. He was with Com Dev Wireless, Dunstable, UK, and was a visiting faculty at the University of Kansas. He is currently a professor with the Department of Electrical Engineering, Indian Institute of Technology Kanpur. His current research interests include antenna analysis, microwave measurements, microwave circuits, radio-frequency identification, and computational electromagnetics.

https://doi.org/10.1017/S1759078718001605 Published online by Cambridge University Press